

# Motion Control Design of Small-Scale Lunar Jumping Robot

Yicheng XU<sup>a</sup>, Zhangli HOU<sup>a</sup>, Weijun WANG<sup>b</sup> and Zhinan ZHANG<sup>a,1</sup>

<sup>a</sup>*School of Mechanical Engineering, Shanghai Jiao Tong University, Shanghai 200240*

<sup>b</sup>*Shanghai Institute of Aerospace System Engineering, Shanghai 201109*

ORCID ID: Yicheng XU <https://orcid.org/0009-0005-9454-0837>

Zhangli HOU <https://orcid.org/0009-0006-8719-964X>

Zhinan ZHANG <https://orcid.org/0000-0002-5868-7840>

Weijun WANG <https://orcid.org/0009-0003-4626-735X>

**Abstract.** Exploring the moon has always been a dream of humanity. For lunar exploration, there is an urgent need for legged jumping robots that are suited to the lunar environment. These robots are currently at the cutting edge of academic research. However, the moon's low gravity and uneven terrain impose high technical demands on these robots' jumping capabilities. As of now, there are no known robots capable of executing such jumps on the moon. This paper presents a motion control algorithm specifically designed for a small-scale lunar jumping robot. The algorithm's feasibility is verified through Adams-Simulink coupled simulation. Based on these simulation results, the control algorithm is implemented in a physical robot, and subsequent jumping experiments demonstrate that the robot can achieve stable and slope-adapted jumping motions in a low-gravity environment.

**Keywords.** Jumping robot, motion control, slope changes

## 1. Introduction

With the development of aerospace technology, China plans to conduct manned lunar landings before 2030 [1]. In this regard, the use of human-machine collaborative exploration technologies has great practical value. For example, by operating lunar robots, it will be easier for astronauts to obtain data and information in complex terrain areas that are difficult to reach, which can expand the scope of lunar exploration effectively. Because of the low gravity and complex terrain on the moon [2,3], legged jumping has energy-saving advantages and is more capable of crossing obstacles than rolling, walking, and running [4].

Many jumping robot prototypes with different shapes have been developed, such as Festo bionic kangaroo [5], MSU running and jumping robot [6], and mini cheetah [7]. However, most are only adapted for takeoff from flat and hard surfaces. The single-legged vertical jumping robot Salto [8] can achieve inclined takeoff, but it is unsuitable for low-gravity environments and cannot maintain a stable static state. It has been found that there is almost no report currently available on legged jumping robots that can adapt to lunar environments. The ability to jump stably on sloping terrains has proven to be a

---

<sup>1</sup> Corresponding Author: Zhinan ZHANG, E-mail: zhinanz@sjtu.edu.cn.

significant challenge in this field. In this paper, we construct a set of motion control algorithms adapted to slope changes with hierarchical control, providing a reference for human-machine cooperation during manned lunar landings.

## 2. Mechanism and motion control design

This section presents the mechanism design of the lunar jumping robot, as well as the hierarchical motion control framework, as a preparation for subsequent simulation experiments.

### 2.1. Jumping mechanism

As shown in Figure 1, the jumping robot adopts a symmetrical jumping leg configuration, with two motors separately controlling energy storage and posture adjustment. Through a transmission mechanism, the motor inputs torque and controls two legs to rotate in the opposite direction synchronously, thereby compressing the legs. A tension spring is installed at the knee joints of the legs, which stretches and stores energy when the legs are compressed, and recovers and releases energy when the legs are extended. By releasing the spring's energy, robots are able to take off. Additionally, a swing rod is positioned at the center of mass to adjust the posture of the robot body, maintaining its balance during jumping.

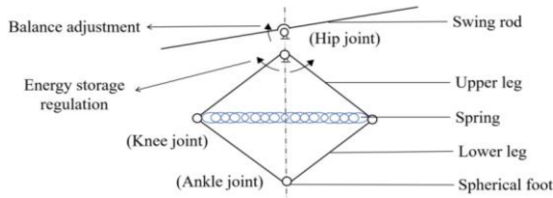


Figure 1. Jumping leg configuration.

### 2.2. Jumping motion control framework

To improve the energy utilization efficiency of the jumping process, the robot is designed for continuous jumps. Consequently, the Central Pattern Generators (CPG) algorithm [9,10], which can generate rhythmic motion directly, could match the control of the continuous jumping motion. The CPG algorithm has been developed for a long time [11,12] and applied to quadruped robots [13,14] and biped hopping robots [15]. The CPG control is also suitable for switching between different motion modes when adapting to various slopes. However, since each neuron of the rhythm generator and pattern generator in the CPG algorithm contains activation functions and integration, the calculation in the control process is rather complex, requiring considerable computational resources. The proposed framework retains the hierarchical structure of the CPG algorithm, simplifies the mathematical formulation of its neuronal components, and enhances its computational efficiency.

We build a robot motion control framework by combining the PD control algorithm and the CPG hierarchical control concept, as shown in Figure 2. The control framework includes three parts: the top perception layer, the intermediate processing layer, and the end output layer.

(1) The top perception layer: The force at the end of the foot is received and compared with the threshold to distinguish whether the current state is the landing phase or the airborne phase.

(2) The intermediate processing layer: The angle and upper-level signals are received to determine specific control objectives in the current state, aiming to achieve continuous jumps on different slopes.

(3) The end output layer: The upper-level signals are detected and converted for proportional-derivative (PD) control and other necessary transformations, with corresponding outputs being provided for the electronic control drive components. This process involves tracking the control targets and driving the hip joint motor and the swing rod motor.

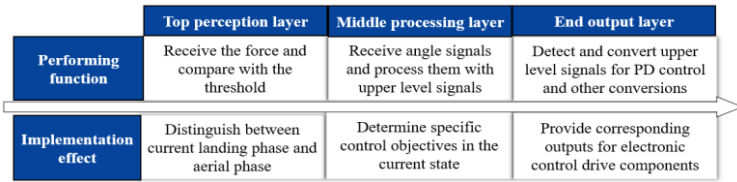


Figure 2. Algorithm diagram of continuous jumping hierarchical control.

### 3. Jumping simulation

Based on the robot's mechanism design and motion control framework, in this section, we conduct Adams-Simulink coupling simulations step by step, from jumping straight up on the flat ground to jumping forward on the flat ground and jumping forward on the slopes. To improve the performance of the robot motion, we further optimize the parameters of the control algorithm by analyzing the simulation outcomes.

#### 3.1. Simulation of jumping in place

In Adams software, we construct a dynamic environment based on the robot's mechanism design in section 2.1. The driving input parameters are defined as the hip joint's torque and the swing rod's angular velocity. The mass and inertia of each model component are specified, and their motions are confined within the vertical plane. Through one worm and two worm gears, the torque is applied symmetrically to both hip joints, ensuring that the two joints can be driven synchronously. Additionally, the inherent self-locking feature of the worm and worm gears prevents the robot's legs from oscillating during the airborne phase.

As shown in Figure 3, the use of slope input signals and attitude PD control can achieve a single stable jump and maintain a stable posture in place throughout the jumping process. A continuous jump cycle is initiated with the highest point position after takeoff. During the subsequent jumping cycles, the drive signal of the hip joint is provided to achieve energy compensation when landing. At the same time, the swing rod maintains the body attitude angle near 0° by constantly adjusting the balanced posture, ultimately achieving a stationary periodic jump.

The variation in jumping height over time is illustrated in Figure 4. The simulation results verify that the robot can achieve continuous jumping by periodically compressing

the leg to supplement energy, providing a reference for setting hip joint torque in subsequent simulations.

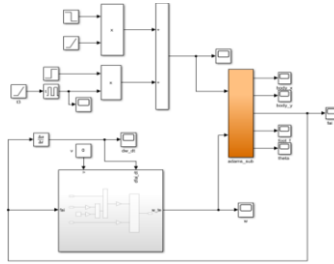


**Figure 3.** Simulink control block diagram of jumping in place.

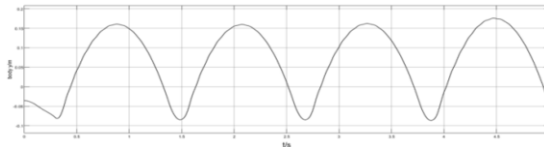


**Figure 4.** Continuous jumping height variation graph.

### 3.2. Simulation of jumping forward

Based on the feedback signals from sensors and the hierarchical control framework in Section 2, the control block diagram is designed, integrating the control of the top perception layer, the intermediate processing layer, and the end output layer. The Simulink control block diagram for simulating continuous marching motion on the flat ground is shown in Figure 5.

In the dynamics simulation module, the input signals for the swing rod's angular velocity are divided into four parts:

- (1) The first part: rotation signals cooperating with the takeoff motion.
- (2) The second part: signals given by the end output layer under the support phase.
- (3) The third part: signals given by the end output layer under the swing phase.
- (4) The fourth part: compensation signals input to prevent the aircraft body from tilting too much under the influence of the aforementioned signals.

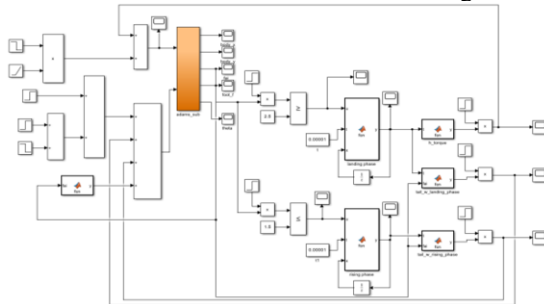


**Figure 5.** Simulink control block diagram of jumping forward.

After parameter adjustment, continuous forward jumping on the flat ground has a good effect. The complete jumping simulation schematic is shown in Figure 6.

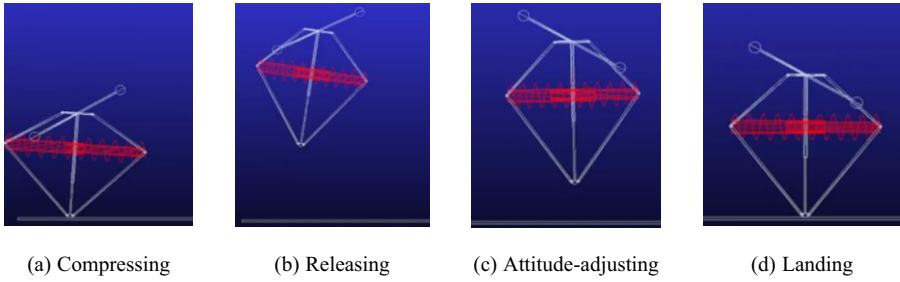


Figure 6. Simulation schematic of continuous jumping motion on the flat ground.

### 3.3. Simulation of jumping on the slope

Based on the motion simulation of continuous forward jumping on the flat ground, we adjust the robot's forward inclination angle during the takeoff process as well as the backward inclination angle during the landing process, which can make the robot adapt to the slope. Using the control block diagram in section 3.2, we modify the ground slope of the modeling diagram to  $\pm 15^\circ$  in Solidworks and further adjust the attitude control parameters to obtain the jumping height diagram for uphill and downhill, as is shown in Figure 7. Simulation tests show that the robot's maximum jumping height is 35 cm, and it can reach a forward velocity of approximately 12 cm/s, which basically meets the requirements of sports indicators.

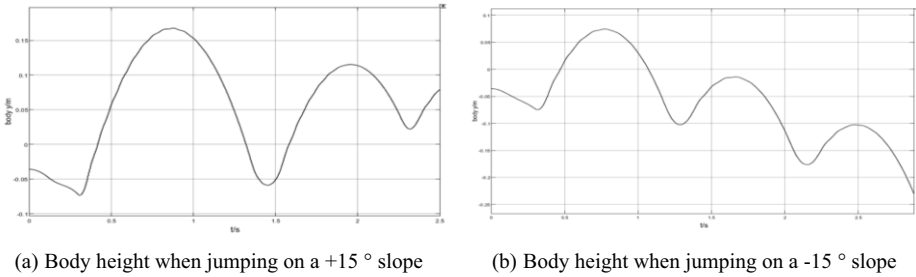


Figure 7. Graph of the body height when jumping on a  $\pm 15^\circ$  slope.

## 4. Motion control deployment

Based on the Adams-Simulink coupling simulation test results, the feasibility of the motion control algorithm framework is determined. The corresponding electronic control hardware is selected for the physical robot, and a hardware control framework is constructed. Multiple experiments are conducted to verify the jumping effect.

### 4.1. Hardware control framework

The electrical control hardware components are connected and assembled, as shown in Figure 8. The control board measures the current posture through the built-in IMU and receives the foot's force signal through the GPIO/INPUT port. With the signals processed, the motors are controlled to rotate through electrical adjustment, and the swing rod is

controlled. Besides, the electromagnetic clutch is controlled through the GPIO/OUTPUT port communication.

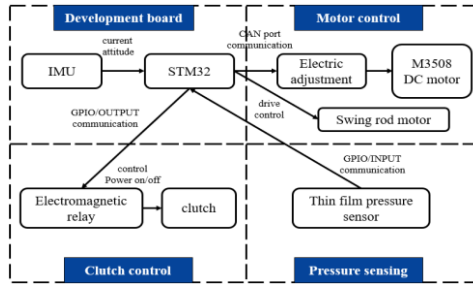


**Figure 8.** Electrical Control Hardware Connection Diagram.

#### 4.2. Jumping test

With the aid of the lunar environment simulating system, three tests of the jumping robot are conducted in sequence, as shown in Figure 9.

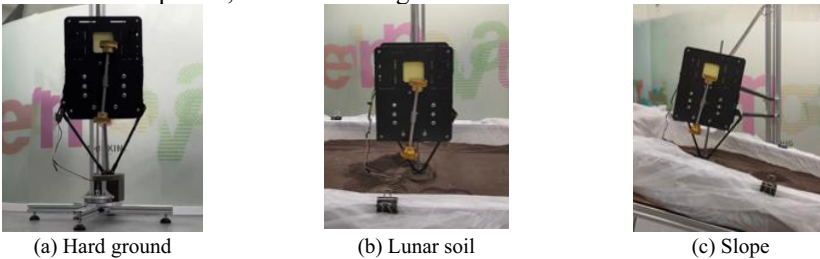


**Figure 9.** Jumping robot experiments.

In the experiments, the robot achieves continuous jumping on the hard flat ground, the lunar flat ground, and the lunar slope in the low gravity simulation environment. Due to the friction of the mechanical system and the noise of the motion control system, there is a small gap between the experiment and simulation results in the jumping height. Besides, experiments demonstrate that the sensitivity and threshold of the foot-end pressure sensors largely influence the robot's state perception capabilities. To enhance the robot's reliability during motion, we adjust its center of mass to a position below the rotational joint, ensuring that its stable equilibrium can be maintained in a horizontal posture. Overall, the robot demonstrates a satisfactory jumping performance.

## 5. Conclusions

In response to the demand for human-machine cooperation in lunar exploration, this paper presents the motion control design for a small-scale lunar jumping robot. A hierarchical control framework is constructed, containing the top perception layer, the intermediate processing layer, and the end output layer. Adams-Simulink coupling simulation tests are performed to verify the feasibility of the control strategy. The motion control algorithm is deployed on the physical robot, and relevant jumping tests are conducted, demonstrating that the hierarchical control algorithm developed in this paper achieves a good implementation effect over the robot's continuous jumping, enabling the

robot to jump stably in the simulated lunar environment. This study explores the locomotion patterns of compact lunar rovers, offering a blueprint for the future development of exploration robots intended for manned lunar missions. We will also further refine the implementation of balance recovery mechanisms and concurrently explore the enhancement of the three-dimensional jumping motions.

## Acknowledgment

This study is financially supported by the Industry-University-Research Cooperation Fund of the Eighth Research Institute of China Aerospace Science and Technology Corporation (No. USSCAST2022-15).

## References

- [1] MALLAPATY S. China set to retrieve first Moon rocks in 40 years. *Nature*. 2020 Nov; 587(7833):185-6, doi: <https://doi.org/10.1038/d41586-020-03064-z>.
- [2] NIKSIRAT P, DACA A, SKONIECZNY K. The effects of reduced-gravity on planetary rover mobility. *The International Journal of Robotics Research*. 2020 Jun; 39(7):797-811, doi: <https://doi.org/10.1177/027836492091394>.
- [3] THOESSEN A, MARVI H. Planetary surface mobility and exploration: A review. *Current Robotics Reports*. 2021 Sep; 2(3):239-49, doi: <https://doi.org/10.1007/s43154-021-00056-3>.
- [4] BURDICK J, FIORINI P. Minimalist jumping robots for celestial exploration. *The International Journal of Robotics Research*. 2003 Jul; 22(7-8):653-74, doi: <https://doi.org/10.1177/02783649030227013>.
- [5] GRAICHEN K, HENTZELT S, HILDEBRANDT A, KÄRCHER N, GAIßERT N, KNUBBEN E. Control design for a bionic kangaroo. *Control Engineering Practice*. 2015 Sep; 42:106-17, doi: <https://doi.org/10.1016/j.conengprac.2015.05.005>.
- [6] ZHAO J, YAN W, XI N, MUTKA MW, XIAO L. A miniature 25 grams running and jumping robot. In2014 IEEE International Conference on Robotics and Automation (ICRA) 2014 May; 5115-5120, doi: <https://doi.org/10.1109/ICRA.2014.6907609>.
- [7] HALDANE DW, PLECNİK MM, YIM JK, FEARING RS. Robotic vertical jumping agility via series-elastic power modulation. *Science Robotics*. 2016 Dec; 1(1):eaag2048, doi: <https://doi.org/10.1126/scirobotics.aag2048>.
- [8] KATZ B, DI CARLO J, KIM S. Mini cheetah: A platform for pushing the limits of dynamic quadruped control. In2019 international conference on robotics and automation (ICRA). 2019 May; 20:6295-6301, doi: <https://doi.org/10.1109/ICRA.2019.8793865>.
- [9] IJSPEERT AJ. Central pattern generators for locomotion control in animals and robots: a review. *Neural networks*. 2008 May; 21(4):642-53, doi: <https://doi.org/10.1016/j.neunet.2008.03.014>.
- [10] LIU C, WANG D, CHEN Q. Central pattern generator inspired control for adaptive walking of biped robots. *IEEE Transactions on Systems, Man, and Cybernetics: Systems*. 2013 Feb; 43(5):1206-15, doi: <https://doi.org/10.1109/TSMC.2012.2235426>.
- [11] FUKUOKA Y, MIMURA T, YASUDA N, KIMURA H. Integration of multi sensors for adaptive walking of a quadruped robot. Proceedings of IEEE International Conference on Multisensor Fusion and Integration for Intelligent Systems, MFI2003. 2003 September; 21-26, doi: <https://doi.org/10.1109/MFI-2003.2003.1232572>.
- [12] KIMURA H, FUKUOKA Y. Adaptive dynamic walking of a quadruped robot on irregular terrain by using neural system model. Proceedings. 2000 IEEE/RSJ International Conference on Intelligent Robots and Systems (IROS 2000). 2000 August; 2:979-984, doi: <https://doi.org/10.1109/IROS.2000.893146>.
- [13] XIE J, MA H, WEI Q, AN H, SU B. Adaptive Walking on Slope of Quadruped Robot Based on CPG. 2019 2nd World Conference on Mechanical Engineering and Intelligent Manufacturing (WCMEIM). 2019 February; 487-493, doi: <https://doi.org/10.1109/WCMEIM48965.2019.00103>.
- [14] ZHANG D, ZHENG W, YANG Y, FANG T. CPG-Based Gait Control Method for Quadruped Robot Jumping Movement. 2021 7th International Conference on Control, Automation and Robotics (ICCAR). 2021 June; 41-45, doi: <https://doi.org/10.1109/ICCAR52225.2021.9463469>.
- [15] WANG T, GUO W, LI M, ZHA F, SUN L. CPG Control for Biped Hopping Robot in Unpredictable Environment[J]. 2012 March; 9(1):29-38, doi: [https://doi.org/10.1016/s1672-6529\(11\)60094-2](https://doi.org/10.1016/s1672-6529(11)60094-2).